Synthesis Approach to the Determination of Optimal Waste Blends under Uncertainty

Prosenjit Chaudhuri and Urmila Diwekar
Center for Energy and Environmental Studies, Dept. of Engineering and Public Policy, Carnegie Mellon University, Pittsburgh, PA 15213

The generalized approach to the problem of synthesis under uncertainty is to formulate it as a stochastic optimization problem that involves optimization of a probabilistic function obtained by sampling over uncertain variables. The computational burden of this approach can be extreme and depends on the sample size used for characterizing the parametric uncertainties. A new and efficient approach for stochastic process synthesis is presented. The goals are achieved through an improved understanding of the sampling phenomena based on the concepts derived from fractal geometry. A new algorithm for stochastic optimization based on these concepts to accelerate the process of synthesis under uncertainty is presented. Apart from the benchmark HDA synthesis problem, a real-world problem of synthesizing optimal waste blends is analyzed to test the applicability of this novel approach in addressing the general problem of synthesis under uncertainty. The solution of this real-world large-scale synthesis problem is presented under uncertainty through the application of the new stochastic annealing algorithm, which takes into consideration novel sampling methods used in probabilistic analysis of process models.

Introduction

Environmental objectives have placed additional requirements on process data and models coupled with the need for sophisticated simulation technology to quantify the impact of pollution prevention options. However, a number of barriers still must be overcome to fully realize the use of these simulation technologies for pollution assessment and prevention. For example, the number of available/possible technology options to address environmental problems has increased significantly as a result of several in-house and federally funded R&D initiatives over the past decade. Thus, a large array of technologies are now available or are under development for emission control. This poses a bewildering problem of selection and optimization of emission control systems or processes, development of analysis and design tools that address the full range of alternative approaches. Furthermore, uncertainties are inherent in the early stages of new process developments and need to be explicitly characterized to fully understand the risks as well as payoffs of alternative systems. The main goal of this article is to address the general problem of process synthesis (that is, selection of optimal process configuration) under uncertainty with applications to environmental control technologies. This goal will be explicitly illustrated through a real-world environmental problem—the selection of optimal blends to dispose high-level radioactive waste when uncertainties exist in the waste composition and in the physical model of the blending procedure.

In general, the approaches to process synthesis may be classified as one of the following: the thermodynamic approach (Linnhoff, 1981); the evolutionary methods (Nishida et al., 1981); the hierarchical approach, based on intuition and judgment (Douglas, 1988); and the optimization or algorithmic approach (Grossmann, 1985; Friedler et al., 1995; Painton and Diwekar, 1994). These approaches, although different in principle, provide promising directions for process synthesis research, and each one brings different advantages to this field. This article concentrates on the optimization approach to process synthesis, which is more amenable to interfacing with the simulators and generalization. Figure 1a shows

Correspondence concerning this article should be addressed to U. Diwekar.

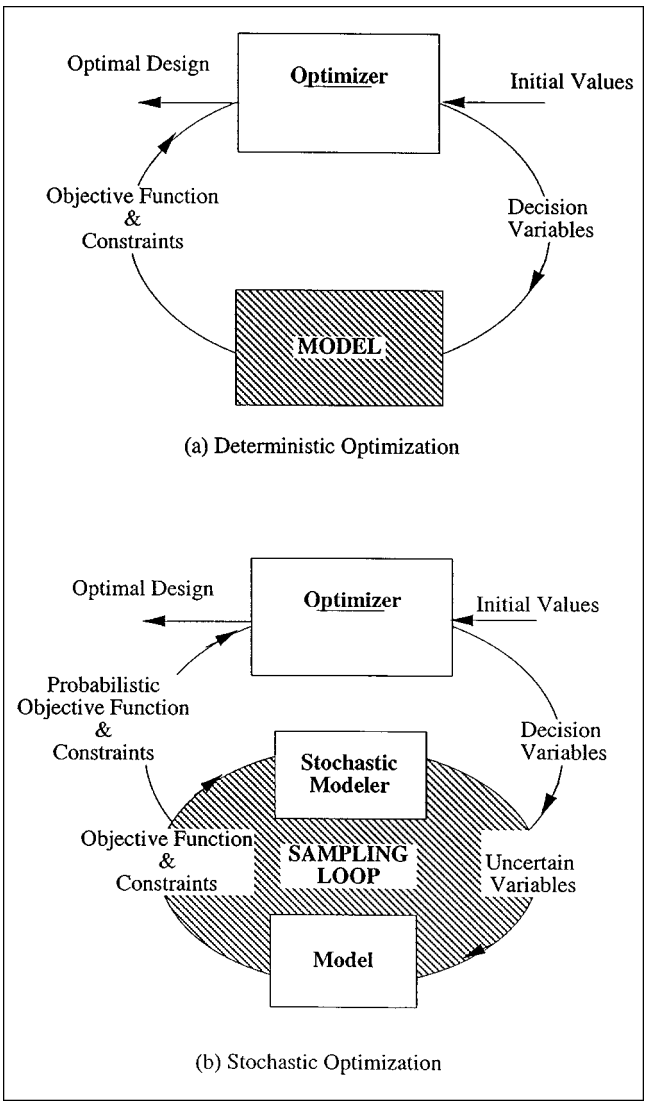

Figure 1. (a) Optimization and (b) stochastic optimization framework.

this optimization approach to process synthesis where the optimizer iteratively determines the decision variables consisting of discrete and continuous variables. The discrete variables denote the existence or absence of units, while the continuous variables represent flows, operating conditions, and design variables.

Conventional optimization of chemical processes are deterministic in nature. The fundamental difference between conventional modeling and the new alternative of integrated environmental technologies, is the problem of uncertainties. Uncertainties arise primarily since the available performance data are scant and the technical as well as the economic parameters are not well established for processes that are in the conceptual stages of development. Moreover, many of the environmental processes are poorly understood and accurate predictive models do not exist. The deterministic performance models in conventional simulators cannot be used for risk or safety evaluations. A systematic framework to analyze uncertainties (Diwekar and Rubin, 1991) is a key step in this regard and promises to overcome some of the difficulties encountered with deterministic simulators. This probabilistic or stochastic modeling procedure involves (1) specifying the uncertainties in key input parameters in terms of probability distributions, (2) sampling the distribution of the specified parameter in an iterative fashion, and (3) propagating the effects of uncertainties through the process flow sheets and applying statistical techniques to analyze the results.

A major bottleneck in the stochastic modeling framework is the computational intensity of the recursive sampling. Synthesis under uncertainty adds further complexity to the stochastic modeling, as it involves stochastic optimization procedure. Figure 1b shows the stochastic optimization procedure, where the deterministic model in Figure 1a is replaced by the stochastic model. Thus the stochastic optimization procedure (synthesis under uncertainty) involves two recursive loops: (1) the inner sampling loop, and (2) the outer optimization loop. Therefore, it is desirable to reduce the computational intensity of these two loops and their interactions for their applicability to large-scale synthesis problems.

Recently, a sampling technique referred as Hammersley sequence sampling (HSS) has been proposed that was shown to exhibit better ''homogeneity'' over the multivariate parameter space (Diwekar and Kalagnanam, 1997). In this context, homogeneity is defined as the ability to produce a uniform distribution of points covering the entire sample space such that the overall distribution is more representative of the population (Wozniakowski, 1991). Further, for this new sampling technique, it was found that the number of samples required to converge to the different performance measures (such as mean, variance or fractiles) of an output random variable, subject to input uncertainties, is lower compared to Monte Carlo or Latin hypercube sampling techniques. This rapid ''convergence'' property of Hammersley sequence sampling has important implications for stochastic modeling of processes, suggesting that precise estimates of any probabilistic function are achievable by taking into consideration a smaller sample size. This efficient sampling can be used for the inner sampling loop to enhance the computational efficiency of the stochastic synthesis framework.

The stochastic annealing algorithm, proposed in the earlier work (Painton and Diwekar, 1995; Chaudhuri and Diwekar, 1996), is an algorithm designed to efficiently optimize a probabilistic objective function and is a good candidate for the outer optimization loop. The algorithm manipulates the sample size automatically, reducing the computational bottleneck of the stochastic synthesis problem. This is achieved by augmenting the real objective function with a penalty term that incorporates the error bandwidth for the probability measure. However, the success of this algorithm depends on the accurate characterization of the error-band width of the inner sampling loop. This article presents a procedure for the characterization of the error bandwidth for the novel and efficient sampling technique, Hammersley sequence sampling (HSS) (Diwekar and Kalagnanam, 1997), based on the self-affinity and scaling properties of the error with the sample size. The characterization of the error bandwidth allows one to use this new sampling technique for the inner loop in the framework for synthesis under uncertainty. It is shown that this new capability is able to improve the performance of

stochastic annealing to a large extent, reducing the computational intensity of stochastic synthesis considerably (as it has been shown that the accurate characterization of the error bandwidth is critically important in defining a more realistic penalty term in the stochastic annealing algorithm, so that faster convergence to the optimum is achievable). This is illustrated by revisiting the HDA synthesis problem presented earlier (Chaudhuri and Diwekar, 1996) and through the solution of a large-scale environmental problem: the determination of optimal waste blends from a high-level radioactive site where uncertainties exist in model parameters and waste composition.

The article is organized as follows: the second and third sections provide the necessary background for the new variant of the stochastic annealing algorithm. The second section describes the general stochastic annealing algorithm for the synthesis of processes under uncertainty. The third section presents the general sampling techniques, illustrates the convergence properties, and compares the error bandwidth for Monte Carlo and Hammersley sequence-sampling techniques. The fourth section is devoted to the new variant of stochastic annealing. In this section the HDA synthesis problem analyzed by several researchers in the past is revisited to illustrate the computational efficiency of the new algorithm. Finally, the fifth section is dedicated to the case study of the large-scale optimal waste-blend synthesis problem.

Stochastic Annealing: Penalty-Function Formulation

In general, the optimization approach to process synthesis involves (a) formulation of a conceptual flow sheet incorporating all the alternative process configurations (superstructure) and (b) identification of an optimal design configuration based on optimal structural topology and the optimal parameter level settings for a system to meet specified performance and cost objectives (Grossmann, 1990). Once the superstructure is known, optimization algorithms can be used to solve the synthesis problem. Mixed-integer nonlinear programming (MINLP) algorithms are commonly used to obtain the optimal structure as well as optimal design. The implementation of MINLP synthesis capability in a sequential modular simulator (SMS) poses challenging problems due to the ''black box'' nature of sequential modular simulators (Diwekar et al., 1992; Diwekar and Rubin, 1993). Furthermore, the MINLP process synthesis capability encounters difficulties when functions do not satisfy convexity conditions, for systems having many possible configurations (leading to large combinatorial explosion), and/or when the solution space has discontinuities.

The alternative to MINLP optimization is to use simulated annealing (SA) (Kirkpatrick et al., 1983). Although simulated annealing is computationally intensive compared to MINLP synthesis, it circumvents the problems associated with an MINLP synthesizer. SA is a recently developed probabilistic method for combinatorial optimization based on ideas from statistical mechanics (Kirkpatrick et al., 1983). The analogy in simulated annealing is the behavior of physical systems in the presence of a heat bath: in physical annealing, all atomic particles arrange themselves in a lattice formation that minimizes the amount of energy in the substance, provided the initial temperature (T_{init}) is sufficiently high and the cooling is carried out slowly. At each temperature, T, the system is allowed to reach thermal equilibrium, which is characterized by the probability (Pr) of being in a state with energy E given by the Boltzmann distribution:

$$Pr(E) = \frac{1}{Z_t} e^{-E/K_b T}, \tag{1}$$

where K_b is Boltzmann's constant (1.3806×10^{23} J/degrees K) and $1/Z_t$ is a normalization factor.

In simulated annealing, the objective function (usually cost) becomes the energy of the system. The goal is to minimize the cost/energy. Simulating the behavior of the system then becomes a question of generating a random perturbation that displaces a ''particle'' (moving the system to another configuration). If the configuration S representing the set of the decision variables θ that results from the move has a lower energy state, the move is accepted. However, if the move is to a higher energy state, the move is accepted according to the Metropolis criteria [accepted with probability $= (1/Z_t) \times e^{-E/K_b T}$] (van Laarhoven and Aarts, 1987). This implies that at high temperatures, a large percentage of uphill moves are accepted. However, as the temperatures gets colder, a small percentage of uphill moves is accepted. After the system has evolved to thermal equilibrium at a given temperature, the temperature is lowered and the annealing process continues until the system reaches a temperature that represents ''freezing'' ($T = T_{\text{freeze}}$). The equilibrium detection at each temperature is a function of the maximum allowable moves at each temperature, N_T, or accept/reject limits N_{acc}/N_T. Thus simulated annealing combines both iterative improvement in local areas and random jumping to help ensure that the system does not get stuck in a local optimum. Although, the original SA algorithm was not designed to handle constraints or infeasibilities, there are various ways of dealing with this problem. For example, one can use explicit penalties for constraint violation (Painton and Diwekar, 1994), or use infeasible path optimization, or use a coupled simulated annealing–nonlinear programming (SA–NLP) approach where the problem is divided into two levels, similar to the MINLP algorithms described earlier. The outer level is SA, which decides the discrete variables. The inner level is NLP for continuous variables and can be used to obtain feasible solution to the outer SA (Narayan et al., 1996).

Stochastic annealing: a variant of simulated annealing for synthesis under uncertainty

The SA algorithm described earlier is used for deterministic synthesis problems. The stochastic annealing algorithm, proposed in earlier work (Painton and Diwekar, 1995; Chaudhuri and Diwekar, 1996), is an algorithm designed to efficiently optimize a probabilistic objective function. In the stochastic annealing algorithm, the optimizer (Figure 1b) not only obtains the decision variables but also the number of samples required for the stochastic model. (By ''stochastic annealing'' we refer to the annealing of an uncertain or stochastic function. It must be realized that the simulated annealing algorithm is inherently a stochastic algorithm, since

the moves are determined probabilistically. For our purposes, however, we are referring to the annealing of a deterministic objective function simply as simulated annealing.) Furthermore, it provides the trade-off between accuracy and efficiency by selecting an increased number of samples as one approaches the optimum.

The new objective function in stochastic annealing therefore consists of a probabilistic objective value P and the penalty function, which is represented as follows:

$$\min Z(\cos t) = P(x, u) + b(t)\epsilon_p. \qquad (2)$$

In the preceding equations, the first term represents the real objective function, which is a probabilistic function in terms of the decision variables x and uncertain variables u, and all other terms following the first term signify the penalty function consisting of the weighting function $b(t)$ $(= b_o/k^t)$ and the error bandwidth, ϵ_p (as a function of number samples). The weighting function $b(t)$ can be expressed in terms of the annealing temperature levels, t, while k is an empirical constant (such as 0.001). The functional dependence on the weight of the temperature level is controlled by these constants, namely b_o and k, which may be different from one problem to another. At high temperatures, the sample size can be small, since the algorithm explores the functional topology or the configuration space, to identify regions of optima. As the system gets cooler, the algorithm searches for the global optimum; consequently, it is necessary to take more samples to get more accurate and realistic objectives/costs. Thus, $b(t)$ increases as the temperature decreases.

The stochastic annealing algorithm minimizes the CPU time by balancing the trade-off between computational efficiency and solution accuracy by the introduction of a penalty function in the objective function. This is necessary, since at high temperature the algorithm is mainly exploring the solution space and does not require precise estimates of any probabilistic function. The algorithm must select more samples, as the solution is near the optimum. The weight of the penalty term, as mentioned before, is governed by $b(t)$ and is based on the annealing temperature.

HDA synthesis

Application of this algorithm for the expected-value function, using the approximate error-bandwidth given by classic statistics, is very encouraging (Painton and Diwekar, 1995; Chaudhuri and Diwekar, 1996). The latter article, presents the process synthesis of a benchmark process in chemical engineering—The hydro alkylation of toluene (HDA) process —as a test problem for the stochastic annealing algorithm. The HDA process has been studied extensively by Douglas and others, starting from the hierarchical approach to process synthesis (Douglas, 1988; Kocis and Grossmann, 1989; Diwekar et al., 1992). The problem that was presented by Chaudhuri and Diwekar (1996) involved selecting the optimal configuration and optimal design of the HDA process when there are uncertainties in the cost parameters. In order to illustrate the computational efficiency that can be achieved using the stochastic annealing algorithm, which automatically selects the optimum number of samples, the process flow sheet was also run using simulated annealing with fixed sample size. The stochastic annealing was able to attain the optimal design configuration obtained using simulated annealing with a fixed sample size, but the stochastic annealing algorithm achieved 80% savings in CPU time using the results from the central limit theorem. Further, it provided an automated, efficient approach to stochastic synthesis. This new, innovative synthesis algorithm therefore holds great promise in the synthesis of large-scale complex chemical processes under uncertainty. The proposed new sampling technique can enhance the computational efficiency further. However, the success of this algorithm depends on the accurate characterization of the error bandwidth in terms of the penalty term (as depicted in Eq. 2). The central limit theorem from the classic statistics is only applicable to Monte Carlo techniques and for the evaluation of the expected value. Although this algorithm was implemented in the context of Monte Carlo sampling, the algorithm in the present form is not applicable to non−Monte Carlo techniques such as the new Hammersley sequence-sampling technique presented in the next section. This is because in stochastic annealing, the cooling schedule is used to decide the weight on the penalty term for imprecision in the probabilistic objective function. The choice of a penalty term, on the other hand, must depend on the error bandwidth of the function that is optimized, and must incorporate the effect of the number of samples. The characterization of the error bandwidth is not possible for non−Monte Carlo techniques. Hence in this article we present a new variant of SA. An approach based on fractal dimension provides the penalty term for this new variant.

Role of Convergence for Different Sampling Techniques

Sampling techniques play a critical role in stochastic modeling of processes. The sampled values for the uncertain parameters must be generated in a manner that ensures that they are random and homogeneous over the multivariate parameter space, and truly representative of the population. It is essential at this stage to present some of the highlights of the different sampling techniques in order to describe the fractal dimension approach for quantifying statistical errors. In the subsequent section, the sampling techniques used in stochastic experiments are discussed, followed by an illustration of the statistical error and the key convergence properties of the sampling techniques.

Common sampling techniques

A stochastic optimization problem involves integrals of any probabilistic function. Hence a sampling technique that provides a representative sample from the multivariate probability distribution is crucial in obtaining true performance statistics for optimization. A general approach is to generate a sequence of n sample points on a k-dimensional hypercube, assuming a uniform $(U(0,1))$ distribution. One of the most widely used sampling techniques for sampling from a probability distribution is the Monte Carlo sampling technique, which is based on a pseudo-random generator to approximate a uniform distribution, $U(0,1)$, with n samples. The specific values for each input variable are selected by inverse

transformation over the cumulative distribution function (Ang and Tang, 1984). A Monte Carlo sample also has the important property that the successive points in the sample are independent. The main advantage of Monte Carlo sampling lies in the fact that the results from any Monte Carlo simulation can be treated using classic statistical methods; thus results can be presented in the form of histograms and methods of statistical estimation. A critical observation, based on classic statistics is that, on an average, the error ϵ of the approximation for the mean is of the order $O(n^{-1/2})$ and is not dependent on the number of variables.

In most applications, the actual relationship between successive points in a sample has no physical significance, hence the independent/randomness of a sample for approximating a uniform distribution is not critical (Knuth, 1973). In such cases, uniformity properties play a central role in sampling techniques, and constrained or stratified sampling techniques are more appealing (Morgan and Henrion, 1990). Latin hypercube sampling (LHS) is one form of stratified sampling that can yield more precise estimates of the distribution function (Iman and Shortencarier, 1984). In Latin hypercube sampling, the range of each uncertain parameter X_i is subdivided into nonoverlapping intervals of equal probability. One value from each interval is selected at random with respect to the probability density in the interval. The n values thus obtained for X_1 are paired in a random manner (equally likely combinations) with n values of X_2. These n values are then combined with n values of X_3 to form n-triplets, and so on, until n k-tuplets are formed. The main drawback of this stratification technique is that it is uniform in one dimension and does not provide uniformity properties on a k-dimensional hypercube. Further, for Latin hypercube sampling, sample scenarios and outcomes are random, but not completely independent. Consequently, this implies that classic statistical methods are not applicable for analyzing any probability function such as the mean, fractile, or the variance for the sampling error manifested through the error bandwidth.

An efficient sampling technique based on Hammersley points has been developed that provides a faster convergence rate than commonly used techniques (Diwekar and Kalagnanam, 1997). This sampling technique uses the Hammersley points to uniformly sample a unit hypercube, and uses the inverse transformation over the joint cumulative probability distribution to provide a sample set for the variables. This sampling design based on Hammersley points has better uniformity properties, since it uses an optimal design scheme for placing n points on a k-dimensional hypercube.

Convergence properties and error bandwidth of sampling techniques

This section presents the convergence properties and the error bandwidth associated with different sampling techniques, qualitatively. One strategy for determining the convergence properties of different sampling techniques is to ascertain the sampling accuracy, that is, the number of samples required by any sampling scheme to converge for any probability function, for example, the mean or the variance. It has been observed that the number of samples required for converging to within 1% of the mean or variance for Hammersley sequence sampling technique is of a factor of 3 to

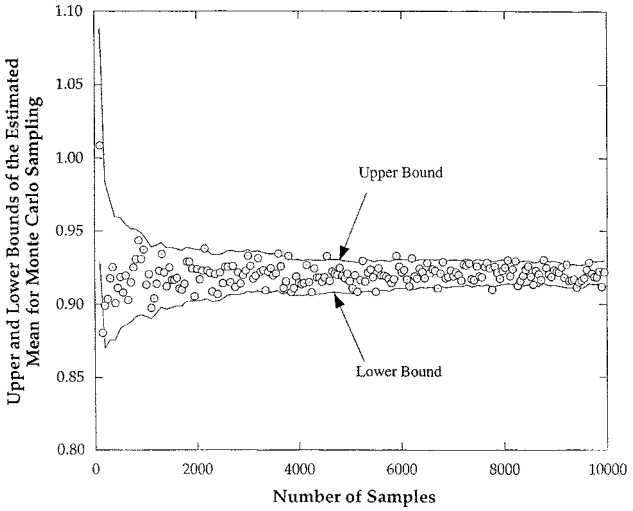

Figure 2. Upper and lower bounds of the estimated mean (95% confidence interval) for Monte Carlo sampling based on classic statistics.

100 lower than Latin hypercube and Monte Carlo sampling techniques (Diwekar and Kalagnanam, 1997). This suggests that the Hammersley sequence is an efficient sampling scheme that can circumvent the computational burden in stochastic modeling and synthesis. Classic statistical methods provide good estimates for the bounds for truly random Monte Carlo sampling and are not applicable to other less random sampling techniques. Figures 2 and 3 show the upper and lower bounds based on the true mean and the true standard deviation (both estimated at 10,000 samples), characterizing the error bandwidth of the estimated mean of a quadratic function of two uncertain parameters [$f(x_1, x_2) = x_1^2 + x_2^2$; x_1 is uniform with $U(0.1, 1.0)$, and x_2 is uniform with

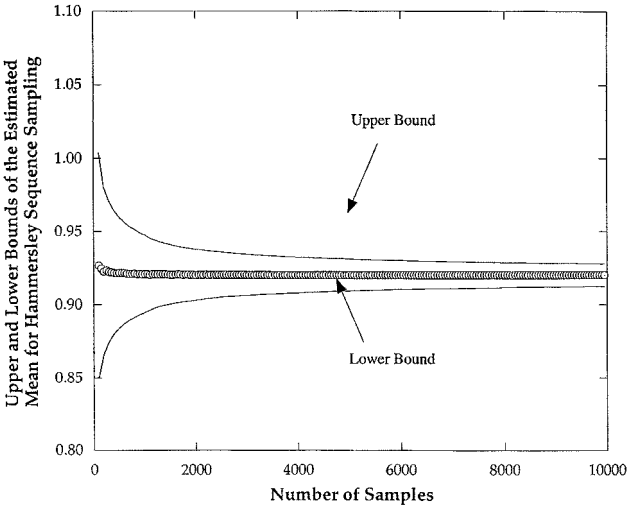

Figure 3. Upper and lower bounds of the estimated mean (95% confidence interval) for Hammersley sequence sampling based on classic statistics.

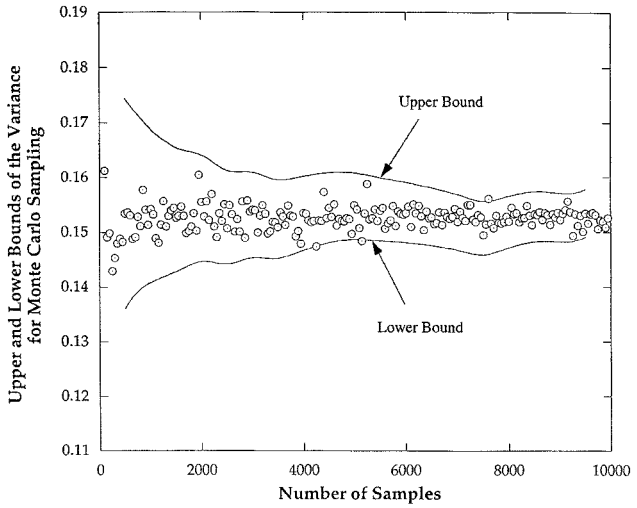

Figure 4. Upper and lower bounds of the estimated variance (95% confidence interval) for Monte Carlo sampling based on classic statistics.

$U(0.1, 1.0)$] for Monte Carlo and Hammersley sequence sampling at 95% confidence levels. It is clearly evident that classic methods to characterize the error bandwidth for any confidence level for Hammersley sequence sampling overestimate the bounds. A similar trend is also observed for the bounds on the variance (Figures 4 and 5). Based on the assumption that the true probability distribution is normal, chi-square estimates for the error bandwidth for a 95% confidence level provide true bounds for Monte Carlo sampling and overestimated bounds for Hammersley sequence sampling. These figures show conclusively that there is a need to characterize precise estimates of the error bandwidths for the improved sampling techniques, since it has important implications on the sampling accuracy in stochastic modeling, synthesis, and uncertainty analysis. In the next subsection we discuss how self-affinity and scaling properties can be used to characterize the error bandwidth for Hammersley sequence sampling.

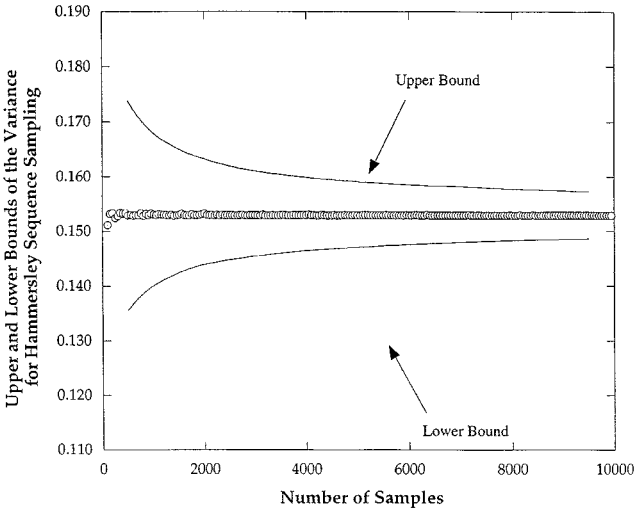

Figure 5. Upper and lower bounds of the estimated variance (95% confidence interval) for Hammersley sequence sampling based on classic statistics.

Self-affinity and scaling properties of the error bandwidth

The previous section illustrated how classic statistics overestimate the error bandwidth for non−Monte Carlo techniques. In the following sections, an approach is outlined to quantify the error bandwidths for any probabilistic function, based on the self-affinity and scaling properties of similar structural patterns shown by many natural phenomena.

Based on the structure of speech waveforms (Pickover and Khorasani, 1985) and acoustic signals (Morgos and Sun, 1990), which show similar irregular patterns as the error associated with the sample techniques, it is possible to draw an analogy between the structure of speech waveforms or signals and the error bandwidth of sampling techniques. For example, parametric test signals exhibit random fluctuations with time, just as the error due to sampling techniques exhibit random fluctuations with the sample size. Figure 6 shows the relative error bandwidth of a probability function for different sample sizes. The characteristic probability function shown here is the mean for a quadratic function [$f(x_1, x_2) = x_1^2 + x_2^2$] of two uncertain parameters, x_1 [Uniform $(0.1, 1.0)$] and x_2 [Uniform $(0.1, 1.0)$]. One can visualize a box whose height (representing the relative error) scales in a statistical self-similar fashion with the sample size. A comparison of the number and nature of peaks in the two adjacent boxes shows that the adjacent boxes exhibit the same ''irregular'' scaling behavior of the error bandwidth with the sample size. The concept of statistical scale invariance is observable (similar to the characteristics of the speech waveform and parametric test signals), where each of these boxes are self-similar (or self-affine) in an average sense. Analogous to the speech waveforms, where acoustic properties scale invariantly with time, in this case, the error bandwidth scales invariantly with the sample size.

In light of the preceding discussion, a scaling relationship is proposed between the error bandwidth and the sample size

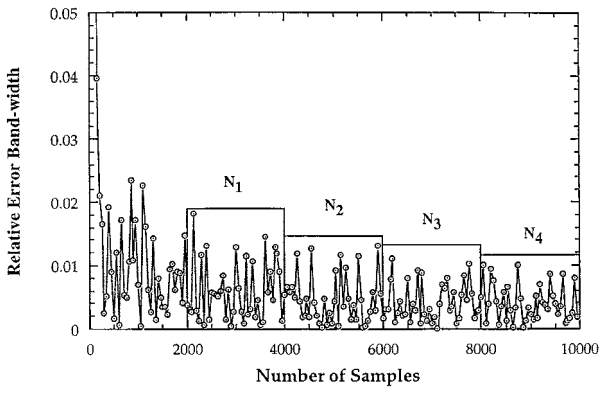

Figure 6. Relative error bandwidth shows self-affine properties and scales with the sample size.

as:

$$\text{Error bandwidth} \sim n^d, \tag{3}$$

where $\sim$ is interpreted as "scales as," and d is the exponent that is characteristic of different sampling techniques. Pickover and Khorasani (1985) have also pointed out that a good exercise to test for self-similarity is to plot the scaling relationship in a log-log plot. If the phenomena have self-similar properties, then the line will be remarkably straight, suggesting a probable fractal nature (Mandelbrot, 1983). Studies that show the similarity of the error bandwidth to fractal objects are presented elsewhere (Diwekar, 1999).

Error characterization of Hammersley sequence sampling

This section illustrates the methodology for characterizing the error bandwidths for the new sampling technique, Hammersley sequence sampling. The same approach was also applied to the Monte Carlo technique to compare the relationship of the error bandwidth with the sample size obtained using the proposed methodology and classic statistics.

In this case, the error bandwidth ϵ is defined, as the relative absolute error expressed as a percentage:

$$\epsilon = \frac{(x_i - x_{\text{conv}})}{x_{\text{conv}}} \times 100, \tag{4}$$

where x_i is any estimate of the probability function, and x_{conv} is the estimate of the probability function after convergence at higher samples, and reflects the actual value of any probability measure.

A large matrix of tests, including the type of function, type of distribution, and the number of uncertain parameters, was designed to study the relationship of the error bandwidth with the sample size for different sampling techniques. The matrix structure involved the following:

- *Functions.* Five different types of functions were used as outlined below:

Function type 1: Linear additive:

$$f(x_1, x_2, \ldots, x_r) = \sum_{i=1}^{r} x_i \qquad r = 2, \ldots, 10$$

Function type 2: Multiplicative:

$$f(x_1, x_2, \ldots, x_r) = \prod_{i=1}^{r} x_i \qquad r = 2, \ldots, 10$$

Function type 3: Quadratic:

$$f(x_1, x_2, \ldots, x_r) = \sum_{i=1}^{r} x_i^2 \qquad r = 2, \ldots, 10$$

Function type 4: Exponential:

$$f(x_1, x_2, \ldots, x_r) = \sum_{i=1}^{r} x_i \exp(x_i) \qquad r = 2, \ldots, 10$$

Table 1. Error Characterization for the Mean and Variance for Monte Carlo Sampling

	X_1 (log), X_2 (log)		X_1 (norm), X_2 (norm)		X_1 (unif), X_2 (unif)	
			Mean			
Function	H'	R^2	d_f	R^2	H'	R^2
Type 1	−0.57	0.90	−0.63	0.93	−0.64	0.95
Type 2	−0.55	0.97	−0.51	0.99	−0.47	0.99
Type 3	−0.53	0.98	−0.53	0.95	−0.53	0.96
Type 4	−0.54	0.99	−0.54	0.99	−0.54	0.99
Type 5	−0.51	0.99	−0.60	0.99	−0.62	0.99
			Variance			
Function	H'	R^2	H'	R^2	H'	R^2
Type 1	−0.75	0.99	−0.75	0.99	−0.65	0.99
Type 2	−0.68	0.97	−0.68	0.97	−0.62	0.99
Type 3	−0.56	0.98	−0.56	0.98	−0.44	0.99
Type 4	−0.51	0.96	−0.51	0.96	−0.54	0.99
Type 5	−0.64	0.99	−0.64	0.99	−0.74	0.99

Function type 5: Logarithmic:

$$f(x_1, x_2, \ldots, x_r) = \sum_{i=1}^{r} \log(x_i) \qquad r = 2, \ldots, 10$$

where the x_i are the uncertain parameters described by the probability distributions.

- *Distributions.* Three types of distributions were selected to characterize the uncertainties in the input variables x_i. The first one is skewed (lognormal), while the last two are symmetric (normal and uniform).

The validity of the proposed relation for the error bandwidth and the sample size (Eq. 3) can be shown through a log-log plot of the error bandwidth, characteristic of each of the self-affine adjacent boxes and the sample size. If Eq. 3 holds true, then the log-log plot will yield a straight line. Tables 1, 2 and 3 present the results for the error bandwidth for both the mean and variance with respect to different functions and different distributions for Monte Carlo and Hammersley sequence sampling.

For the quadratic function (function type 3) mentioned previously, log-log plots of the error bandwidth are plotted

Table 2. Error Characterization for the Mean and Variance for Hammersley Sequence Sampling

	X_1 (log), X_2 (log)		X_1 (norm), X_2 (norm)		X_1 (unif), X_2 (unif)	
Function	H'	R^2	H'	R^2	H'	R^2
			Mean			
Type 1	−2.07	0.97	−2.12	0.96	−1.99	0.97
Type 2	−2.17	0.89	−2.26	0.89	−1.97	0.91
Type 3	−2.12	0.97	−2.15	0.96	−2.02	0.97
Type 4	−2.28	0.93	−2.35	0.90	−2.12	0.93
Type 5	−2.47	0.91	−1.76	0.85	−1.89	0.91
			Variance			
Type 1	−1.85	0.93	−1.28	0.95	−1.26	0.97
Type 2	−1.34	0.88	−1.63	0.91	−1.45	0.93
Type 3	−2.09	0.95	−1.19	0.99	−1.21	0.99
Type 4	−1.88	0.96	−1.24	0.99	−1.47	0.93
Type 5	−2.95	0.99	−1.64	0.90	−1.57	0.93

Table 3. Error Characterization for the Mean and Variance for Hammersley Sequence Sampling for a Range of Uncertain Parameters and for Two Different Functional Forms

Function Type 1			Function Type 4		
No. of Uncertain Pars.	H'	R^2	No. of Uncertain Pars.	H'	R^2
		Mean			
2	−1.99	0.97	2	−2.12	0.93
3	−2.05	0.99	3	−2.10	0.95
4	−1.91	0.99	4	−1.89	0.98
5	−1.71	0.99	5	−1.79	0.99
6	−1.63	0.98	6	−1.58	0.99
7	−1.81	0.98	7	−1.62	0.99
8	−1.79	0.99	8	−1.77	0.98
9	−1.91	0.98	9	−1.87	0.98
10	−1.86	0.97	10	−1.78	0.98
		Variance			
2	−1.26	0.97	2	−1.47	0.93
3	−1.16	0.99	3	−1.29	0.96
4	−1.48	0.99	4	−1.32	0.96
5	−1.76	0.99	5	−1.32	0.99
6	−1.61	0.99	6	−1.32	0.99
7	−1.44	0.99	7	−1.39	0.99
8	−1.33	0.99	8	−1.19	0.99
9	−1.37	0.98	9	−1.01	0.97
10	−1.62	0.99	10	−1.30	0.99

against the sample size for both the mean (Figure 7) and variance (Figure 8) for Monte Carlo and Hammersley sequence sampling based on two uncertain parameters, x_1 [x_1 is uniform, $U(0.01, 1.0)$] and x_2 [x_2 is uniform, $U(0.01, 1.0)$]. The scaling relationship is obvious from the two figures, which exhibit good coefficients of determination (R^2 values), suggesting its fractal nature. It is worth mentioning that a simple curve fit of the error bandwidth vs. number of samples did not yield good R^2 values, proving conclusively that the relationship between the error bandwidth and the sample size is

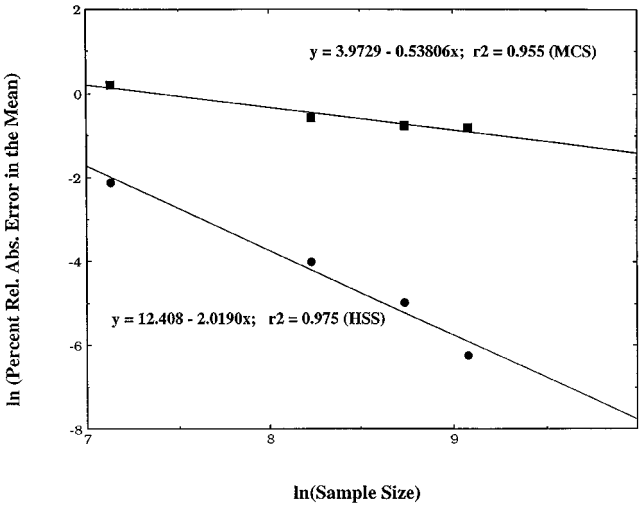

Figure 7. Characterization of the error bandwidth associated with the mean for Monte Carlo and Hammersley sequence sampling.

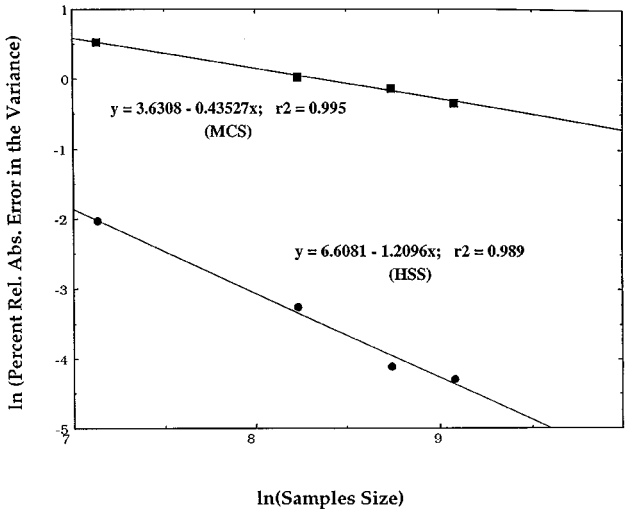

Figure 8. Characterization of the error bandwidth associated with the variance for Monte Carlo and Hammersley sequence sampling.

not a power-law relationship, and both self-affinity and the scaling properties must be taken into account to obtain good linear fits that suggest its fractal nature. The exponent H' is obtained from the slope of the linear relationship, which is different for the mean and variance and for Monte Carlo and Hammersley sequence-sampling techniques. Note, however, that this model may not be applicable for extremely low sample sizes (that is, N tending to 1). The higher dimensions obtained for the mean and the variance for Hammersley sequence sampling are consistent with the fact that probability functions such as the mean and the variance converge at many fewer samples for Hammersley sequence sampling than for Monte Carlo sampling.

It is seen that the characterization of the error bandwidth for the mean based on the self-affine fractal characterization in the case of the Monte Carlo technique is almost identical to the relationship predicted by classic statistics. It may be recalled that classic statistics predict that the error bandwidth of mean for Monte Carlo techniques should scale as $N^{-0.5}$, where N is the sample size. The experimentally determined exponent for the relationship between the error bandwidth and the number of samples is almost -0.5, with good linear fits, indicating that the proposed model characterizes the error bandwidth for Monte Carlo sampling technique fairly well.

It is also observed, based on experiments with several uncertain parameters for Hammersley sequence sampling and for Monte Carlo sampling, that the exponent H' is independent of the number of uncertain parameters, the output relationship, or the type of uncertainty distributions. This is important, since it shows that this method of characterizing the error bandwidth is robust, and quantifies the behavior of the error bandwidth with the sample size globally. It was observed that the Latin hypercube sampling technique did not consistently predict the same exponent when the number of variables, functional relationship, or distributions are changed.

New Variant of Stochastic Annealing

Based on the results presented in the earlier tables, the error bandwidth for the mean in the case of Hammersley sequence sampling scales with N, the sample size, as $N^{-1.8}$. Consequently, the penalty term in the stochastic annealing algorithm for the mean in the case of Hammersley sequence sampling is defined as

$$\epsilon_P = \left(\frac{b_0}{k^t}\right)_{HSS} N_{samp}^{-1.8},$$

where, b_0 and k are empirical constants, t is the corresponding temperature level, which decreases as the annealing proceeds, and N_{samp} is the number of samples. It may be recalled that the penalty term in the stochastic annealing algorithm for the mean in the case of Monte Carlo sampling is given by

$$b(t)\epsilon_p = \left(\frac{b_0}{k^t}\right)_{MCS} N_{samp}^{-0.5}.$$

The empirical constants are determined through experimentation such that the penalty term is less than 5% of the real objective function, as mentioned earlier, and they are problem-dependent. The next paragraph illustrates the computational efficiency of the stochastic annealing algorithm implemented with the Hammersley sequence sampling, for which the error bandwidth was characterized based on the self-affinity and scaling properties mentioned previously.

HDA problem revisited

In Chaudhuri and Diwekar (1996), the HDA process was synthesized in the presence of uncertainties, where the sampling method was based on Latin hypercube sampling. As mentioned previously, the error bandwidth based on classic statistical methods are overestimated for non−Monte Carlo techniques. In this case, the synthesis of the HDA process was performed using the new variant of stochastic annealing based on Hammersley sequence sampling for which the error bandwidth was characterized using a scaling relationship obtained from the self-affinity and scaling properties of the error bandwidth with the sample size.

Table 4 illustrates the computational savings of the stochastic annealing algorithm with Hammersley sequence sampling incorporating the error bandwidth characterization. The results show that this capability improves the performance of the stochastic annealing algorithm, thereby reducing the computational expense (by approximately 33%) of stochastic synthesis. This is particularly critical for large, complex process flow sheets, which can now be synthesized in computationally affordable time. The second part of this article presents a large-scale problem of synthesizing optimal waste blend where the new algorithm reduced the computational time from 4 days to 18 hours.

In order to show the applicability of the stochastic annealing algorithm with the fractal dimension approach for quantifying the error bandwidth, it is necessary to apply the algorithm to a large-scale problem. The problem chosen for this exercise pertains to the synthesis of optimal waste blends under uncertainty.

Table 4. Comparison of the Results for the HDA Problem Using Stochastic Annealing Implemented with Latin Hypercube and Hammersley Sequence Sampling Techniques*

	Algorithm	
Decision Variables	Stochastic Annealing HSS-Scaling Relationship	Stochastic Annealing LHS-Classic Relationship
$y1$	1	1
$y2$	0	0
$y3$	0	0
$y4$	1	1
Conversion	0.619	0.609
Reactor temp.	867 K	867 K
Furnace temp.	894 K	893 K
Molar flow rate (hydrogen feed)	249 kmol/h	253 kmol/h
Molar flow rate (toluene feed)	126 kmol/h	127 kmol/h
CPU time	10,736 s	14,516 s
Maximized Profit, $/yr	660	650

*For Hammersley sequence as opposed to Latin hypercube sampling, the error bandwidth was accurately characterized using a robust approach based on self-affinity and scaling properties of the error with the sample size.

Synthesizing Optimal Waste Blends under Uncertainty

This section illustrates the application of the stochastic annealing algorithm, which takes into consideration more efficient sampling techniques for stochastic modeling and synthesis of chemical processes, on the determination of optimal waste blends encountered in a classic, real-world environmental problem. This problem relates to the Hanford site in southwestern Washington that produced nuclear materials using various processes for nearly 50 years. The byproducts of many of these processes resulted in the production of hazardous and radioactive wastes of widely varying composition. Although the site ceased to be a manufacturing facility a few decades ago, ''Hanford was reborn in 1989 with a new mission—to be the flagship site leading environmental restoration'' (Illman, 1993). In order to facilitate the cleanup and the restoration process, the wastes were classified into *high-level* and *low-level* fractions to be immobilized for future disposal. The cleanup effort led to the investigation and identification of new technologies for the reclamation of radioactive waste for disposal or long-term storage.

At present, it is desired that the high-level liquid waste be converted to borosilicate glass for storage in a geologic repository, since radioactivity does not leak easily through glass. This process, called vitrification, requires that certain conditions related to ''processibility'' and ''durability'' be satisfied, so that the conversion is achievable. The processibility conditions ensure that during the processing stage, the glass melt has properties, such as viscosity, electrical conductivity, and liquidus temperature, that lie within ranges known to be acceptable for the vitrification process. The durability considerations ensure that the resultant glass meets the quantitative criteria for storage in a repository.

The Hanford site has 177 tanks [capacity ranging from 50,000 gal to 1 million gal (190 kL to 3.8 ML)] containing radioactive waste. During the vitrification process, it is required that the wastes in the tanks and appropriate glass forms (frit) are mixed and heated in a melter to form glass that satisfies the constraints. The main objective is to add the minimum amount of frit and still achieve the reclamation of the wastes. This has major implications: first, this keeps the frit costs to a minimum, and second, the amount of waste per glass log formed is maximized, thus keeping the waste disposal costs to a minimum. It was realized that the minimum amount of frit would be used if all the high-level wastes in the tanks were combined to form a single feed to the vitrification process. Further, the procedure for finding the minimum amount of frit for a single feed to the vitrification process is also relatively easy. Unfortunately, the large volume of the wastes and the time span over which they need to be processed makes this strategy a nonviable option. Previously, it was established that some of the same benefits can be achieved by forming blends from a set of tanks (Hoza, 1993). The problem, then, is how to divide all the tanks into sets to be blended together (given the tank compositions and the total mass of each tank) such that the minimum amount of frit is required. This problem of determining the optimal waste-blend configuration was studied previously by Narayan et al. (1996) based on data pertaining to a subset of the total number of tanks at the Hanford site, using various techniques including a coupled simulated annealing and nonlinear programming. The study assumed that there are no uncertainties related to the waste composition in the tanks, and in the glass physical property models (Narayan et al., 1996).

As shown in the present study, uncertainties play a critical role in the determination of optimal configuration for these waste blends. The uncertainties are associated with (1) the range of applicability of the glass-property models, and (2) waste composition in the tanks. The waste composition uncertainties primarily arise due to the variability in the composition of the wastes, nonhomogeneity of the tank contents, and poor documentation of the contents of each tank. As Deborah Illman writes:

> ''To make matters worse, wastes are often comingled on the site, unlike most hazardous waste sites. Organic wastes has co-contaminants—heavy metals, fission products, transuranics. And the mixed waste burial trenches, used from 1944–1970, may contain a mind-boggling potpourri including solid sodium, plutonium, pyrophorics, munitions, and other wastes in close proximity to one another. But no one is sure, because the records are poor.''

This leads to a challenging problem of determining the optimal waste-blend configuration subject to the inherent uncertainties in the waste compositions and in the glass physical-property models. The formulation is based on the stochastic optimization framework, and addresses the question as to how uncertainties affect the calculated waste loading and the synthesis of optimal waste blends. It was observed that this exercise of synthesizing optimal waste blends under uncertainty is a computational-intensive problem, requiring several days of CPU time. A novel approach based on stochastic annealing coupled with nonlinear programming (STA–NLP), using an efficient sampling technique yields an optimal solution in 18 hours of CPU time, without any significant loss of solution accuracy.

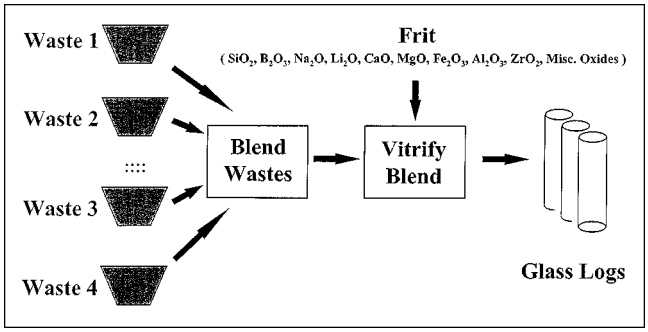

Figure 9. Vitrification process.

Problem description

The vitrification process begins with the blending of different tank wastes to form a blend, which is then pretreated and mixed with the frit in a melter under certain conditions, to produce glass of the desired quality. It must be realized that the term ''frit'' truly refers to a composite, consisting of a mixture of oxides, all of which are present in varied amounts in the original wastes. The components in the frit must be added to the waste blend in proper proportions to produce glass (and therefore must satisfy the ''processibility'' and ''durability'' constraints). Figure 9 shows this vitrification problem.

The blending problem addressed in this section consists of mixing the N different waste sources or tanks to form a discrete number of blends B. It is required that *all* the waste from any given tank must combine with other wastes to form a single blend, each blend containing wastes from N/B sources. The blends must therefore be of equal size (that is, same number of wastes per blend) or alternatively, blends could be formulated to have approximately the same waste masses. These constraints ensure that all the wastes did not go into a single blend (Hoza, 1993). The following section presents the formulation of the deterministic blending problem, which is also the basis for the stochastic optimization formulation for determining the optimal blend configuration in the presence of uncertainties.

Mathematical formulation of the blending problem

Given a set of tanks (N) and the number of blends (B) that needs to be formed, the number of tanks (T) that forms a blend is therefore given by

$$T = \frac{N}{B}. \tag{5}$$

If $w^{(i)}$ is the mass of the ith component in the waste, $f^{(i)}$ the mass of ith component in the frit, and $g^{(i)}$ the mass of the

ith component in glass, the following equality constraints result:

$$g^{(i)} = w^{(i)} + f^{(i)} \tag{6}$$

$$G = \sum_{i=1}^{n} g^{(i)} \tag{7}$$

$$fg^{(i)} = \frac{g^{(i)}}{G}, \tag{8}$$

where G is the total mass of the glass formed, n the total number of components, and $fg^{(i)}$ denotes the fraction of the ith component in the glass. The formation of glass from the blend is governed by several constraints that are briefly described below. A detailed description of the constraints can be found in the Appendix.

- *Individual Component Bounds.* These constraints limit the range of the mass fractions each component can have in the calculated glass composition. For each of the components in glass, lower ($fg_{LL}^{(i)}$) and upper ($fg_{UL}^{(i)}$) limits are specified for each mass fraction:

$$fg_{LL}^{(i)} \le fg^{(i)} \le fg_{UL}^{(i)}. \tag{9}$$

- *Crystallinity Constraints.* These are the multiple-component constraints that limit the combined fractions of different components. There are five such constraints.
- *Solubility Constraints.* These constraints limit the maximum value for the mass fraction of one or a combination of components (such as oxides of noble metals: $Rh_2O_3 + PdO + Ru_2O_3$). They are intended to represent the solubility limits for the specified components and are of the form:

$$fg^{K} \le fg_{UL}^{k}, \tag{10}$$

where k is the solubility component and fg_{UL}^{K} denotes the mass fractions of the particular solubility component.

- *Glass-Property Constraints.* These constraints govern the glass properties such as viscosity, electrical conductivity, and durability. They are of the form:

$$\ln(\text{minpropval}) \le \sum_{i=1}^{n} b_i fg^i + \sum_{i=1}^{n} \sum_{j \ge i} b_{ij} fg^i fg^j \le \ln(\text{maxpropval}) \tag{11}$$

where b_i and b_{ij} are the first-order and second-order coefficients in the model, respectively; fg^i is the mass fraction of component i; and n is the number of components. The minpropval and maxpropval are the lower and upper bounds of the glass property values, respectively.

The objective is to select the combination of the wastes in the tanks that would form each blend so that the total amount of frit is minimized. The combinatorial size of this mixed-discrete-optimization problem increases with the number of wastes and the number of blends (Narayan et al., 1996). The possible number of combinations for a total of N tanks that form B blends, with each blend consisting of T tanks, is given by

$$\text{Possible combinations} = \frac{N!}{B!(T!)^B}. \tag{12}$$

For a small subset (21) of the total number of tanks at the Hanford site to be partitioned into three blends, there are 66,512,160 possible ways to form the three blends. The number of possible configurations of the blends thus poses an overwhelming problem for common search algorithms to determine the optimal blend configuration. The next subsection illustrates the procedure proposed by Narayan et al. (1996) for solving the deterministic problem of finding the optimal blend configuration.

The presence of uncertainties not only increases the computational intensity of the problem, but it also affects the optimal blend configuration. The uncertainties associated with the waste-blending problem is described in Hoza (Hopkins et al., 1994) and in the following paragraphs.

Optimal Waste Loading Under Uncertainty. The uncertainties currently being addressed in the optimal waste-loading problem fall into two categories: property-prediction uncertainty and waste-stream composition uncertainty (Hopkins et al., 1994). In this section, the two sources of uncertainty are briefly described. The characterization of the uncertainties in the model is presented in the next section.

1. *Uncertainties in Waste Composition.* The wastes in the tanks were formed as byproducts in different processes used to produce radioactive materials. Consequently, there is associated with each of these tanks a certain degree of variability. Furthermore, over a period of 40 to 50 years, physical and chemical transformations within a tank have resulted in a nonuniform, nonhomogeneous mixture. Any experimental sample of the waste withdrawn from the tank is not representative of the tank as a whole, which contributes significantly to the uncertainty associated with the waste composition. This is supplemented, to a lesser extent, by the uncertainties associated with the analytical measurements in determining the waste compositions.

2. *Uncertainties in Glass-Property Models.* The glass-property models are empirical equations fitted to the data (that is, glass-property values against glass compositions). Predictions made with a fitted property model are subjected to uncertainty in the fitted model coefficients. The uncertainties result from the random errors in property values introduced during the testing and measurements, as well as the minor lack-of-fit of the empirical model relative to the actual one (Hopkins et al., 1994). Uncertainties in glass-property models reduce the feasible range of the application of the glass-property models, thereby affecting the optimal waste loading.

Characterization of Uncertainties in the Model. This subsection outlines the methodology adopted to characterize the uncertainties in the waste composition and the glass-property models. Since this is a preliminary study, several assumptions have been made to keep the problem manageable and to focus on the key objective; namely, to develop an efficient method for solving this large-scale problem in computationally affordable time, and to illustrate how uncertainties affect the optimal blend configuration. Most of the assumptions

pertain to uncertainties in the waste composition. The assumptions and simplifications used in this work are listed below.

Characterization of Uncertainties in Waste Composition. As mentioned previously, the uncertainties in the waste composition arise from many sources. The assumptions used in this study regarding waste-composition uncertainties are as follows:

- For this study, ''waste composition uncertainty'' is a general term, covering all possible uncertainties in waste-feed composition. These sources include batch-to-batch (within a waste type), sampling within a batch, and analytical uncertainties.
- The only estimate of this ''lumped'' uncertainty in the composition of the waste feed for high-level vitrification was based on the information available (that is, analytical tank composition data).
- There is no bias in the composition estimates; the sample values are distributed about the true mean.
- The derived component mass fractions were assumed to follow normal distributions.
- The uncertainties of the species in the waste were assumed to be relatively independent of each other (that is, uncorrelated).
- The relative standard deviation for each component in a particular waste tank was taken to be representative of all the tanks in the study. This assumption needs to be refined as subsequent data becomes available.

The procedure employed in characterizing the waste composition uncertainties is as follows:

- Based on the mean and the relative standard deviation (RSD) for each component in the tank, normal probability distributions were developed for the individual mass fractions. For a particular tank waste, the range of uncertainty is shown in Table 5.
- The preceding distributions were sampled to develop N_{samp} waste-composition input sets (mass fractions). A stratified sampling technique (Latin hypercube sampling or LHS) (Iman and Shortencarier, 1984), and the novel sampling technique, Hammersley sequence sampling (HSS) (Diwekar and Kalagnanam, 1997), were both used to generate the samples, and to observe the implication of different sampling techniques on the optimum blend configuration and the computational time.
- Given the mass fractions and the total mass of the wastes, the mass fractions were normalized to 1.0.
- The mean of the input waste mass for each component, based on N_{samp} samples of the component mass fractions, was then used in the model run.

Table 5. Mean Mass, RSD, and the Uncertainty Associated with Component Masses for a Pretreated High-Level Waste in a Particular Tank (B-110) at the Hanford Site

Components	Mass Fraction	Mass (kg)	RSD	Uncertainty (kg)
Al_2O_3	0.02002	25,165.1	0.15	$25{,}165.1(1\pm3\times0.15)$
B_2O_3	0.000856	1,075.9	0.13	$1{,}075.9(1\pm3\times0.13)$
CaO	0.011293	14,195.3	0.07	$14{,}195.3(1\pm3\times0.07)$
Fe_2O_3	0.229344	288,285.2	0.04	$288{,}285.2(1\pm3\times0.04)$
Li_2O	—	—	—	—
MgO	0.002687	3,377.6	0.04	$3{,}377.6(1\pm3\times0.04)$
Na_2O	0.080439	101,111.7	0.04	$101{,}111.7(1\pm3\times0.04)$
SiO_2	0.175263	220,305.4	0.04	$220{,}305.4(1\pm3\times0.04)$
ZrO_2	0.000041	51.4	0.12	$51.4(1\pm3\times0.12)$
Other oxides	0.480056	603,429.9	0.056	$603{,}429.9(1\pm3\times0.056)$
Cr_2O_3	0.014986	18,837.4	0.03	$18{,}837.4(1\pm3\times0.03)$
F	—	—	—	—
P_2O_5	0.248923	312,895.9	0.04	$312{,}895.9(1\pm3\times0.04)$
SO_3	—	—	—	—
NobMet	—	—	—	—

Characterization of Uncertainty in Physical-Property Models. The uncertainty in a predicted property value for a given glass composition is defined as (Hopkins et al., 1994):

$$\text{Uncert}_{\text{prop}} = M\left[x^T S x\right]^{0.5} \tag{13}$$

where

M = multiplier, which is usually the upper 95th percentile of a t-distribution ($t_{0.95}(n-p)$], where n is the number of data points used to fit the model and p is the number of fitted parameters (coefficients) in the model
x = glass-composition vector expanded in the form of the model
S = covariance matrix of the estimated parameters (coefficients), that is, b_i and b_{ij}

For nonlinear property models adopted in this study, the usual glass-composition vector x is augmented by second-order terms. For example, if there are two second-order terms, x_1^2 and $x_2 x_4$, the usual composition vector (x_1, ..., x_{10}) becomes (x_1, ..., x_{10}, x_1^2, $x_2 x_4$). The uncertainty expression (Eq. 13) corresponds to a statistical confidence statement on the property model prediction, considered as a prediction of the mean property value for a glass composition x.

The uncertainty defined in Eq. 13 affects the glass property constraints by narrowing the feasible region determined by the glass-property models. The form of the glass-property constraints using this approach is given by

$$\ln(\text{minpropval}) + \text{Uncert}_{\text{prop}} \le \sum_{i=1}^{n} b_i fg^i + \sum_{i=1}^{n}\sum_{j\ge i} b_{ij} fg^i fg^j \le \ln(\text{maxpropval}) - \text{Uncert}_{\text{prop}}, \tag{14}$$

where minpropval and maxpropval are the lower and upper bounds on the glass-property value. It is easily observed that if $\text{Uncert}_{\text{prop}} = 0$, this constraint formulation reduces to Eq. 11, where no uncertainties are associated with the glass-property models.

Solution procedure

The blending process addressed in this article is similar to some of the processing applications in the coal and petroleum industry. A survey of the techniques used to determine the optimal blend configuration in such cases revealed that most of the methods were based on successive linear, integer, and nonlinear programming (Palacios-Gomez, 1980; Lasdon and Warren, 1980; Baker and Lasdon, 1982; Beale, 1978). The highly nonconvex nature of the constraints and the large combinatorial size of the discrete blending problem at hand make it necessary to apply innovative combinatorial opti-

mization techniques so that the optimal blend configuration is determined.

Deterministic Optimization Problem. Narayan et al. (1996) studied the deterministic problem of determining the optimal blend configuration based on 21 tanks and 3 blends, each blend consisting of 21/3 or 7 tanks. The composition of the 21 tanks are presented in Table 6. The approaches adopted by Narayan et al. to study the blending problem were as follows:

- *Heuristic Approach.* In this case, the limiting constraint was identified taking into consideration all (21) tanks. The blends were then formulated such that each blend has the same limiting constraint. If this was achievable, then the frit required would have been the same for the total blend. This approach was found to be very difficult to implement in practice; rather, the blends were formulated so that all blends were near the limiting value of the limiting constraint (Narayan et al., 1996). The minimum frit requirement found using this approach was 11,736 kg of frit.
- *GAMS-Based MINLP Approach.* The GAMS-based MINLP approach was very dependent on the initial conditions for the calculation. The best solution found using this approach was 12,341 kg of frit. The GAMS-based MINLP model failed to find the global optimal solution due to the nonconvexities in the problem structure (Narayan et al., 1996).
- *Coupled Simulated Annealing–Nonlinear Programming Approach (SA-NLP).* Narayan et al. (1996) proposed a two-stage approach based on simulated annealing and nonlinear programming to determine the optimal blend configuration for this problem. The solution procedure for the deterministic problem is shown in Figure 10.

The objective was to select a combination of blends for which the total amount of frit added was minimum. The discrete decision was related to the distribution of the tanks among the three blends, and was generated by the outer loop of the two-stage SA–NLP algorithm. The objective function for the outer loop (SA) was formulated as the minimization of the total mass of the frit over a combination of blends:

$$\min \sum_{j=1}^{B} \sum_{i=1}^{n} f_j^{(i)}, \qquad \text{(SA)} \tag{15}$$

Table 6. Waste Composition Data for the 21 Tank Problem Studied by Narayan et al.

	Fractional Composition of Wastes $w^{(i)}/g^{(i)}$										
Comp.	AY-102	AZ-101	AZ-102	SY-102	SY-101	SY-103	B-103	BY-104	BY-110	C-103	C-105
SiO_2	0.072	0.092	0.022	0.020	0.000	0.019	0.011	0.030	0.040	0.412	0.359
B_2O_3	0.026	0.000	0.006	0.003	0.000	0.000	0.000	0.000	0.000	0.000	0.000
Na_2O	0.105	0.264	0.120	0.154	0.300	0.230	0.100	0.082	0.089	0.006	0.012
Li_2O	0.000	0.000	0.000	0.000	0.000	0.000	0.000	0.000	0.000	0.000	0.000
CaO	0.061	0.012	0.010	0.030	0.007	0.006	0.000	0.141	0.046	0.041	0.044
MgO	0.040	0.000	0.003	0.012	0.000	0.001	0.000	0.000	0.000	0.028	0.026
Fe_2O_3	0.328	0.323	0.392	0.133	0.000	0.039	0.155	0.067	0.051	0.338	0.064
Al_2O_3	0.148	0.157	0.212	0.318	0.659	0.546	0.214	0.344	0.462	0.057	0.372
ZrO_2	0.002	0.057	0.063	0.002	0.000	0.001	0.000	0.007	0.003	0.043	0.004
Other	0.217	0.096	0.173	0.328	0.034	0.159	0.520	0.330	0.309	0.075	0.119
Total	1.000	1.000	1.000	1.000	1.000	1.000	1.000	1.000	1.000	1.000	1.000
Cr_2O_3	0.016	0.007	0.005	0.089	0.002	0.116	0.000	0.000	0.000	0.002	0.005
F	0.006	0.001	0.001	0.005	0.002	0.001	0.000	0.001	0.001	0.000	0.000
P_2O_5	0.042	0.001	0.021	0.088	0.013	0.005	0.037	0.016	0.022	0.013	0.012
SO_3	0.001	0.018	0.009	0.027	0.005	0.002	0.007	0.002	0.003	0.000	0.002
NobMet	0.000	0.000	0.000	0.000	0.000	0.000	0.000	0.000	0.000	0.000	0.000
Waste Mass	59,772	40,409	143,747	359,609	167,510	185,990	6,170	155,473	103,492	85,211	207,127
Comp.	C-106	C-108	C-109	C-111	C-112	S-102	SX-106	TX-105	TX-118	U-107	
SiO_2	0.437	0.001	0.001	0.002	0.001	0.000	0.033	0.010	0.060	0.008	
B_2O_3	0.000	0.000	0.000	0.000	0.000	0.000	0.000	0.000	0.000	0.000	
Na_2O	0.014	0.010	0.007	0.011	0.005	0.337	0.280	0.168	0.425	0.038	
Li_2O	0.000	0.000	0.000	0.000	0.000	0.000	0.000	0.000	0.000	0.000	
CaO	0.046	0.000	0.737	0.426	0.593	0.000	0.000	0.000	0.000	0.000	
MgO	0.031	0.000	0.000	0.000	0.000	0.000	0.000	0.000	0.000	0.000	
Fe_2O_3	0.214	0.206	0.003	0.042	0.002	0.023	0.102	0.167	0.026	0.077	
Al_2O_3	0.168	0.693	0.013	0.256	0.097	0.582	0.388	0.595	0.240	0.650	
ZrO_2	0.008	0.032	0.000	0.007	0.000	0.000	0.000	0.000	0.000	0.000	
Other	0.082	0.058	0.238	0.256	0.302	0.058	0.197	0.060	0.250	0.228	
Total	1.000	1.000	1.000	1.000	1.000	1.000	1.000	1.000	1.000	1.000	
Cr_2O_3	0.004	0.002	0.000	0.000	0.000	0.024	0.020	0.000	0.000	0.000	
F	0.000	0.000	0.000	0.000	0.000	0.000	0.001	0.000	0.004	0.001	
P_2O_5	0.031	0.047	0.003	0.012	0.005	0.006	0.038	0.002	0.159	0.020	
SO_3	0.000	0.000	0.000	0.000	0.000	0.000	0.003	0.001	0.009	0.001	
NobMet	0.000	0.000	0.000	0.000	0.000	0.000	0.000	0.000	0.000	0.000	
Waste Mass	367,165	46,919	53,271	24,485	65,673	36,537	45,273	42,200	412,495	11,504	

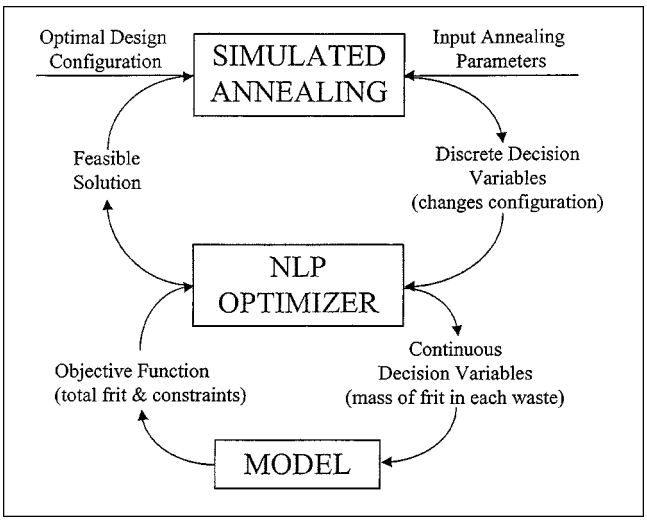

Figure 10. Solution procedure for the SA–NLP algorithm proposed by Narayan et al. for the waste-blending problem (deterministic case).

where $f_j^{(i)}$ is the mass of the ith component in the frit for the jth waste blend, and n and B denote the total number of components, and the given number (3) of blends that needs to be formed, respectively.

Once the blend (j) was fixed, the resultant NLP subproblem, which consisted of a linear objective function and a mixture of linear and nonlinear constraints, was formulated as

$$\min \sum_{i=1}^{n} f^{(i)} \qquad \text{(NLP)}, \tag{16}$$

subject to:

Equality constraints (Eqs. 5–8)
Individual component bounds (Eq. 9)
Crystallinity constraints
Solubility constraints (Eq. 10)
Glass property constraints (Eq. 11).

The combined SA-NLP approach was able to identify an optimal solution (11,028 kg) that was lower than the solution predicted by the heuristic and the GAMS-based MINLP approaches. The optimal solution is presented in Table 7. The optimum using the simulated annealing-NLP approach was verified to be the global optimum using a branch-and-bound strategy. Unfortunately, it was observed that branch and bound was computationally intensive compared to the proposed SA–NLP algorithm (such as branch and bound took 3 days of CPU time, as opposed to 45 min of computational time using the SA–NLP approach on a DEC-ALPHA 400 machine), indicating clearly that the SA–NLP approach can be a promising tool for solving large-scale, computationally intensive, mixed–discrete nonlinear optimization problems.

Stochastic optimization problem

The problem of determining the optimal blend configuration in the presence of uncertainties in the waste composition as well as in the physical property models is posed as a stochastic optimization problem. In the earlier articles, it was shown that stochastic annealing provides an automated, efficient framework for addressing such problems. The stochastic optimization problem requires that the quantities for the waste composition must be represented in terms of their expected values. Thus Eqs. 6–8 are represented as

$$g_e^{(i)} = E[w^{(i)}] + f_e^{(i)} \tag{17}$$

$$G_e = \sum_{i=1}^{n} g_e^{(i)} \tag{18}$$

$$fg_e^{(i)} = \frac{g_e^{(i)}}{G_e}, \tag{19}$$

where the subscript e signifies that the quantities are based on the expected value, and $E[w^{(i)}]$ signifies the expected value of the waste mass of the ith component in the waste.

Similarly, the individual component bounds, crystallinity constraints, solubility constraints, and the glass property constraints are formulated as

$$fg_{LL}^{(i)} \le fg_e^{(i)} \le fg_{UL}^{(i)} \tag{20}$$

$$fg_e^{k} \le fg_{UL}^{k} \tag{21}$$

$$\ln(\text{minpropval}) + \text{Uncert}_{\text{prop}} \le \sum_{i=1}^{n} b_i fg_e^{i} + \sum_{i=1}^{n} \sum_{j \ge i} b_{ij} fg_e^{i} fg_e^{j} \le \ln(\text{maxpropval}) - \text{Uncert}_{\text{prop}}. \tag{22}$$

The approach adopted for this waste-blending problem is based on a coupled STA–NLP technique, which is illustrated

Table 7. Optimal Blend Configuration for the Deterministic Case

Blends	Tank Distribution
Blend 1	3, 4, 5, 6, 8, 9, 20
Blend 2	1, 10, 11, 12, 16, 19, 21
Blend 3	2, 7, 13, 14, 15, 17, 18

	Mass in Frit $f^{(i)}$ (kg)		
Component	Blend 1	Blend 2	Blend 3
SiO_2	293.78	680.950	4550.6
B_2O_3	31.350	2.186	1212.4
Na_2O	38.683	375.06	1130.3
Li_2O	43.890	64.709	302.97
CaO	0.000	11.466	344.20
MgO	0.000	66.866A	485.78
Fe_2O_3	0.000	0.000	502.11
Al_2O_3	0.000	0.000	640.96
ZrO_2	0.000	0.000	0.000
Other	0.000	0.000	250.07

Source: Narayan et al. (1996).

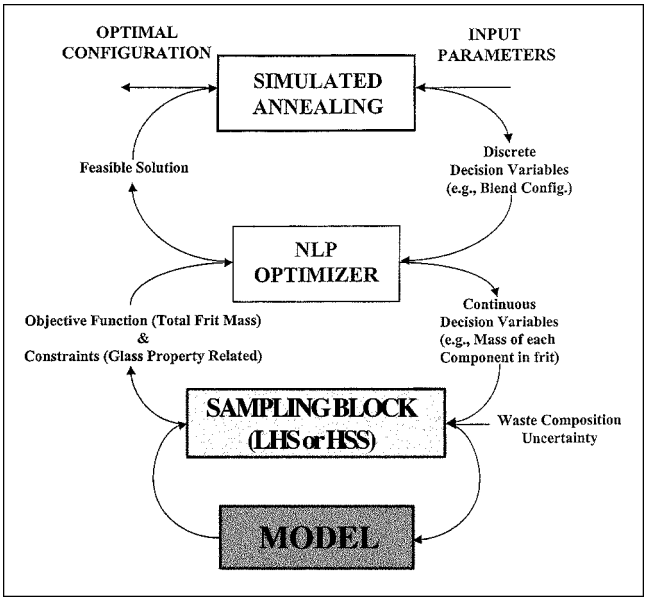

Figure 11. Three-stage stochastic-annealing (STA–NLP) algorithm.

in Figure 11. The solution procedure incorporates a sequence of three loops nested within one another. The inner loop corresponds to the sampling loop, which generates the samples for the mass fractions (or masses) of the different components in the waste, evaluates the mean of the waste mass for each tank, which is then propagated through the model that determines the glass-property constraints. It must be noted that since uncertainties in the glass-property models were incorporated by reducing the feasible region, as mentioned previously, a sampling exercise to account for uncertainties in the property models is not necessary. The loop above the sampling loop is the NLP optimization loop based on successive quadratic programming, a widely used technique for solving large-scale, nonlinear optimization problems. The objective function for the NLP optimizer identifies the minimum amount of frit for a *given* blend configuration based on the expected value of the masses of the components in the waste blend:

$$\min \sum_{i=1}^{n} f_e^{(i)} \qquad \text{(NLP)}, \tag{23}$$

subject to:

Equality constraints (Eqs. 5, 17–18)
Individual component bounds (Eq. 19)
Crystallinity constraints
Solubility constraints (Eq. 20)
Glass-property constraints (Eq. 21),

where, $f_e^{(i)}$ is the composition of the ith-component in the frit based on the expected value of the waste composition, and subject to the uncertainties in the physical-property models.

Finally, the outer loop in the sequence consists of the stochastic annealing algorithm, which predicts the sample size for the recursive sampling loop, and generates the blend configuration such that the total amount of frit is minimum over all the blends:

$$\min \sum_{j=1}^{B} \sum_{i=1}^{n} f_{j_e} \qquad \text{(STA)}, \tag{24}$$

where f_{j_e} is the mass of the ith component in the frit based on the expected values for the waste composition and the uncertainties in the physical-property models for the jth waste blend, and n and B denote the total number of components and the given number (3) of blends that needs to be formed, respectively.

The NLP problem is solved based on the expected value of the objective function, which is obtained from the runs of the model for the different samples at each configuration predicted by the stochastic annealing algorithm. The termination of the entire procedure is governed by the stochastic annealing algorithm and is dependent on the ''freezing'' criterion mentioned in the earlier paper (Chaudhuri and Diwekar, 1996).

Results and discussion

In order to study the effect of the uncertainties in waste composition and in the glass-property models, the stochastic optimization problem of determining the optimal blend configuration was solved using two sampling techniques; namely, Latin hypercube and Hammersley sequence sampling. As mentioned previously, the presence of uncertainties in the waste composition makes this problem highly computationally intensive. In fact, a fixed sample framework for stochastic optimization using 200 samples and Latin Hypercube sampling was unable to converge on an optimal solution in 5 days (total run time was expected to be approximately 20 days), on a DEC-ALPHA 400 machine! This demanded the use of the coupled STA–NLP approach to identify an optimal solution in a reasonable computational time.

The optimal design configuration identified by the coupled STA–NLP approach using Latin hypercube sampling and Hammersley sequence sampling are presented in Tables 8 and 9, respectively. The minimum quantity of frit required using both Latin hypercube and Hammersley sequence sampling is 11,307 kg. Nevertheless, the STA–NLP approach involving Hammersley sequence sampling, for which the error bandwidth was characterized based on a scaling relationship, was found to be computationally less intensive. For example, the STA–NLP technique using Hammersley sequence sampling and improved formulation of the penalty term in the stochastic annealing algorithm, through accurate error bandwidth characterizations based on the scaling relationship, took 18 hours, as opposed to 4 days using Latin hypercube sampling.

It is observed that the presence of uncertainties affect the optimal blend configuration, compared to a deterministic analysis (Table 7), significantly. In fact, given the uncertainties in the waste composition and the physical-property models, the optimal design configuration obtained by Narayan et al. (1996) for the deterministic case, estimates the total frit

Table 8. Optimal Waste Blend Configuration in the Presence of Uncertainties in the Waste Composition and Glass Physical Property Models (Stochastic Case)*

Blends	Tank Distribution
Blend 1	7, 13, 14, 17, 18, 19, 21
Blend 2	4, 5, 6, 8, 9, 16, 20
Blend 3	1, 2, 3, 10, 11, 12, 15

	Mass in Frit $f_e^{(i)}$ (kg)		
Component	Blend 1	Blend 2	Blend 3
SiO_2	356.49	5489.1	923.19
B_2O_3	37.997	826.70	0.6956
Na_2O	51.624	826.74	427.28
Li_2O	51.784	756.86	46.428
CaO	0.000	25.355	5.7003
MgO	0.000	0.000	43.944
Fe_2O_3	0.000	395.51	0.000
Al_2O_3	0.000	1020.0	0.000
ZrO_2	0.000	0.000	0.000
Other	0.000	21.784	0.000

The sampling exercise was performed using Latin hypercube sampling.

requirement to be 12,022 kg. This study reemphasizes the need for characterizing uncertainties in process model for the purpose of determining the optimal design configuration.

Conclusions

Sampling across a multivariate probability distribution is an integral part of stochastic modeling and synthesis. An important aspect of probabilistic modeling is the characterization of the sampling error manifested through the error bandwidth of any output probability function in a simulation experiment. Classical statistics can estimate the error bandwidth associated with the mean and variance for Monte Carlo sampling, and is not applicable to any other sampling techniques. On the other hand, efficient and more uniform sampling techniques exist, for which the error bandwidths have not been characterized in the past. A methodology based on the self-affinity and scaling properties of the error with the sample size has been proposed, and was shown to estimate the error bandwidth more accurately for more uniform sampling schemes. The methodology is robust, and is reasonably independent of the functional forms, probability distributions for the uncertain parameters, and the number of uncertain parameters. This new approach using Hammersley sequence sampling was implemented in the stochastic annealing framework, resulting in increased computational savings. This approach made it possible to solve in a reasonable amount of computational time, the real-world problem of obtaining optimal design configuration of radioactive waste blends to be transformed into glass for long-term storage in a repository. The new capability for stochastic synthesis shows great promise for the synthesis of large-scale processes under uncertainty.

Table 9. Optimal Waste Blend Configuration in the Presence of Uncertainties in the Waste Composition and Glass Physical Property Models (Stochastic Case)*

Blends	Tank Distribution
Blend 1	7, 13, 14, 17, 18, 19, 21
Blend 2	4, 5, 6, 8, 9, 16, 20
Blend 3	1, 2, 3, 10, 11, 12, 15

	Mass in Frit $f_e^{(i)}$ (kg)		
Component	Blend 1	Blend 2	Blend 3
SiO_2	356.81	5489.3	947.63
B_2O_3	38.000	828.07	1.0557
Na_2O	51.741	825.30	427.37
Li_2O	51.817	756.83	55.064
CaO	0.000	25.279	2.1108
MgO	0.000	0.000	14.208
Fe_2O_3	0.000	394.64	0.000
Al_2O_3	0.000	1,020.6	0.000
ZrO_3	0.000	0.000	0.000
Other	0.000	21.590	0.000

The sampling exercise was performed using Hammersley sequence sampling.

Acknowledgments

Funding for this work was sponsored by the National Science Foundation Grant CTS 9613561. The authors gratefully acknowledge the extensive discussions with Professor Rangaranjan Pitchumani, Department of Mechanical Engineering, University of Connecticut, Storrs.

Literature Cited

Ang, A. H. S., and W. H. Tang, *Probability Concepts in Engineering Planning and Design*, Vol. 2, *Decision, Risk and Reliability*, Wiley, New York (1984).

Baker, T. E., and L. S. Lasdon, ''Successive Linear Programming at Exxon,'' Univ. of Texas at Austin, Austin (1982).

Beale, E. M. L., ''Nonlinear Programming Using a General Mathematical Programming System,'' *Design and Optimization Software*, H. J. Greenberg, ed., Sijthoff & Noordhoff, Netherlands (1978).

Chaudhuri, P., and U. M. Diwekar, ''Synthesis Under Uncertainty: A Penalty Function Approach,'' *AIChE J.*, **42**, 742 (1996).

Diwekar, U., ''An Efficient Approach to Optimization under Uncertainty,'' *Ann. Oper. Res.* (1999).

Diwekar, U. M., and J. R. Kalagnanam, ''Efficient Sampling Technique for Optimization Under Uncertainty,'' *AIChE J.*, **43**, 440 (1997).

Diwekar, U. M., and E. S. Rubin, ''Stochastic Modeling of Chemical Processes,'' *Comput. Chem. Eng.*, **15**, 105 (1991).

Diwekar, U. M., I. E. Grossmann, and E. S. Rubin, ''An MINLP Process Synthesizer for a Sequential Modular Simulator,'' *Ind. Eng. Chem. Res.*, **31**, 313 (1992).

Diwekar, U. M., and E. S. Rubin, ''An Efficient Handling of the Implicit Constraints Problem in the ASPEN MINLP Process Synthesizer,'' *Ind. Eng. Chem. Res.*, **32**, 2006 (1993).

Douglas, J. M., *Conceptual Design of Chemical Processes*, McGraw-Hill, New York (1988).

Feder, J., *Fractals*, Plenum, New York (1988).

Friedler, F., J. B. Verga, and L. T. Fan, ''Algorithmic Approach to the Integration of Total Flowsheet Synthesis and Waste Minimization,'' *Chem. Eng. Sci.*, **50**, 1218 (1995).

Grossmann, I. E., ''Mixed-Integer Programming Approach for the Synthesis of Integrated Process Flowsheets,'' *Comput. Chem. Eng.*, **9**(5), 463 (1985).

Grossmann, I. E., ''Mixed-Integer Nonlinear Programming Techniques for the Synthesis of Engineering Systems,'' *Res. Eng. Des.*, **1**, 205 (1990).

Hopkins, D. F., M. Hoza, and C. A. Lo Presti, ''FY94 Optimal Waste Loading Models Development,'' report prepared for U.S. Department of Energy under Contract DE-AC06-76RLO 1830 (1994).

Hoza, M., ''Optimal Waste Loading Models for Vitrification of Hanford High-Level Waste,'' report prepared for U.S. Department of Energy under Contract DE-AC06-76RLO 1830 (1993).

Illman, D. L., ''Researchers Take Up Environmental Challenge at Hanford,'' *Chem. Eng. News*, 9 (July 21, 1993).

Iman, R. L., and M. J. Shortencarier, *A FORTRAN77 Program and User's Guide for the Generation of Latin Hypercube and Random Samples for Use with Computer Models*, NUREG/CR-3624, SAND83—2365, Sandia National Laboratory, Albuquerque, NM (1984).

Kirkpatrick, S., C. Gelatt, and M. Vecchi, ''Optimization by Simulated Annealing,'' *Science*, **220**, 670 (1983).

Kocis, G. R., and I. E. Grossmann, ''A Modeling and Decomposition Strategy for MINLP Optimization of Process Flowsheets,'' *Comput. Chem. Eng.*, **13**, 797 (1989).

Knuth, D. E., *The Art of Computer Programming*, Vol. 1, *Fundamental Algorithms*, Addison-Wesley, Reading, MA (1973).

Lasdon, L. S., and A. D. Warren, ''Survey of Nonlinear Programming Applications,'' *Oper. Res.*, **28**, 1029 (1980).

Linnhoff, B., *Foundations of Computer-Aided Chemical Process Design*, Vol. II, R. S. H. Mah and W. D. Seider, eds., Engineering Foundation, New York, p. 537 (1981).

Mandelbrot, B. B., *The Fractal Geometry of Nature*, Freeman, New York (1983).

Margos, P., and F.-K. Sun, *Measuring the Fractal Dimension of Signals: Morphological Covers and Iterative Optimization*, Tech. Rep. CICS-P-193, Center for Intelligent Control Systems, M.I.T., Cambridge, MA (1990).

Morgan, G. M., and M. Henrion, *Uncertainty— A Guide to Dealing with Uncertainty in Quantitative Risk and Policy Analysis*, Cambridge Univ. Press, Cambridge (1990).

Narayan, V., U. M. Diwekar, and M. Hoza, ''Synthesizing Optimal Waste Blends,'' *Ind. Eng. Chem. Res.*, **35**, 3519 (1996).

Nishida, N., G. Stephanopoulos, and A. Westerberg, ''A Review of Process Synthesis,'' *AIChE J.*, **27**, 321 (1981).

Palacios-Gomez, F. E., ''The Solution of Nonlinear Optimization Problems Using Successive Linear Programming System,'' PhD Thesis, Univ. of Texas at Austin, Austin (1980).

Painton, L., and U. M. Diwekar, ''Synthesizing Optimal Design Configurations for a Brayton Cycle Power Plant,'' *Comput. Chem. Eng.*, **18**, 369 (1994).

Painton, L. A., and U. M. Diwekar, ''Stochastic Annealing Under Uncertainty,'' *Eur. J. Oper. Res.*, **83**, 489 (1995).

Pickover, C. A., and A. Khorasani, *On the Fractal Structure of Speech Waveforms and Other Sampled Data*, Res. Rep. No. 11305, Computer Science Dept., IBM Thomas J. Watson Research Center, Yorktown Heights, NY (1985).

van Laarhoven, P. J. M., and E. H. L. Aarts, *Simulated Annealing: Theory and Applications*, Reidel, Dordrecht, The Netherlands (1987).

Wozniakowski, H., ''Average Case Complexity of Multivariate Integration,'' *Bull. Amer. Math. Soc.*, **24**, 185 (1991).

Manuscript received Dec. 2, 1996, and revision received Feb. 16, 1999.